

# Multifunctional Ionic Liquid-Fe<sub>3</sub>O<sub>4</sub> Core/Chitosan Shell Magnetic Hydrogel for Magnetic Responsive, pH-triggered and Long-Acting Hormone Therapy

Doaa Ragab and Sohrab Rohani\*

Department of Chemical and Biochemical Engineering, University of Western Ontario, London

Submission: November 26, 2015; Published: February 08, 2016

\*Corresponding author: Sohrab Rohani, Department of Chemical and Biochemical Engineering, University of Western Ontario, London, Ontario, Canada, N6A 5B9; Email: sroahni@uwo.ca

## Abstract

Core-shell Chitosan magnetic hydrogels containing encapsulated progesterone were prepared, and their biomedical application as a long acting and magnetic targeted system was evaluated. Magnetic hydrogels were cross-linked at different feed ratios of ionic liquid, and their gel forming ability, magnetic localization and drug release properties were examined. The hydrogels were loaded with progesterone at drug loading percentages ranging from  $30 \pm 2.75$  to  $37.50 \pm 2.85\%$ . The results obtained showed that ionic liquid-Fe<sub>3</sub>O<sub>4</sub> core / chitosan shell magnetic hydrogel exhibited excellent drug encapsulation efficiencies and a sustained drug release profile with a highly controlled initial burst effect. The current study highlights the effect of pH on the loading and release characteristics of the magnetic hydrogel as a result of the change in the network architecture of chitosan. The concentration of ionic cross-linker showed a significant effect on the release profile of progesterone. The approach developed in this work can be potentially used to develop sustained release formulations of progesterone by controlling the chemical configuration of chitosan network.

**Keywords:** Core-shell magnetic nanoparticles; Hydrogel; Chitosan; Controlled drug delivery; *In-vitro* cytotoxicity

## Introduction

Hydrogels have recently attracted much attention because of their versatile therapeutic and biomedical applications [1,2]. Hydrogels are characterized by their 3-D network structure of cross-linked hydrophilic polymer, which can be designed as drug carrier systems for a wide range of drugs such as proteins [3], vaccines [4] and oligonucleotides [5]. The interest of the controlled release applications of hydrogels arises from the tightly cross-linked polymer backbone of hydrogels; which offers a sustained delivery of many therapeutic agents.

Magnetic nanoparticles have attracted much attention in the last few years as carriers for targeted drug delivery systems. Magnetic capsules and magnetic nanoparticles coated with smart polymers have been reported for controlled and localized drug delivery [6-8]. The research on the development of hydrogels for biomedical applications has strongly grown in the last few years [9]. Polysaccharide-based magnetic hydrogels have gained much concern because of their biocompatibility and versatile applications in the areas of biotechnology and biomedicine [10,11].

Comparable systems that have been used for such applications are pH- and temperature- responsive hydrogels. However, a major challenge on developing hydrogel-based drug delivery systems is their high swelling; which results in an uncontrolled degradability [12]. Schillemans et al. [13] investigated the development of anionic and cationic dextran hydrogels as a drug delivery system for protein. The major limitations in this system are the non-homogeneity in drug loading in addition to the high initial burst effect.

The key factors that control the transport of drug molecules from the hydrogel environment to the external release media are important. Therefore, several publications have investigated the effect of surface functionalization on the release characteristics of therapeutic agents from hydrogels drug delivery systems [14-16]. The aforementioned examples demonstrate the major setbacks for the currently developed hydrogels as controlled drug delivery systems; which are (I) High initial burst effect, (II) Poor loading efficiencies and (III) Loss of the coating layer during the release period [17].

Therefore, the fabrication of a heterogeneous structure inside the hydrogel, such as a core-shell structure has been suggested

to control the deteriorating limitations of the outer coating. In addition, the possibility to encapsulate the drug in the inner core as an alternative strategy to control the initial burst effect and to enhance the drug loading efficiencies, has been suggested [17]. Understanding the transport mechanism of water molecules through a hydrogel gives an insight into the drug release profile from their 3D structure. Similarly, the movement of drug molecules to the outside (external release medium) could be also related to the hydrogel swelling rate [18,19].

In this study, we designed a core-shell magnetic hydrogel composed of chitosan-ionic liquid polymer network surrounding the core magnetic  $\text{Fe}_3\text{O}_4$  nanoparticles. The synthesized ionic liquid- $\text{Fe}_3\text{O}_4$  core / chitosan shell magnetic hydrogel displayed a tunable network architecture and superior drug loading functionality. The proposed surface modified hydrogels comprised bi-functional segments: a stable swollen segment of ionic liquid-chitosan (pH-responsive segment) and a magnetic responsive segment ( $\text{Fe}_3\text{O}_4$  core). Based on the selected chitosan network architecture, it was suggested that the controlled drug release profile could result from the electrostatic complexation of the network chains. The controlled drug release profile of progesterone was systematically investigated as a function of variation in the network structure.

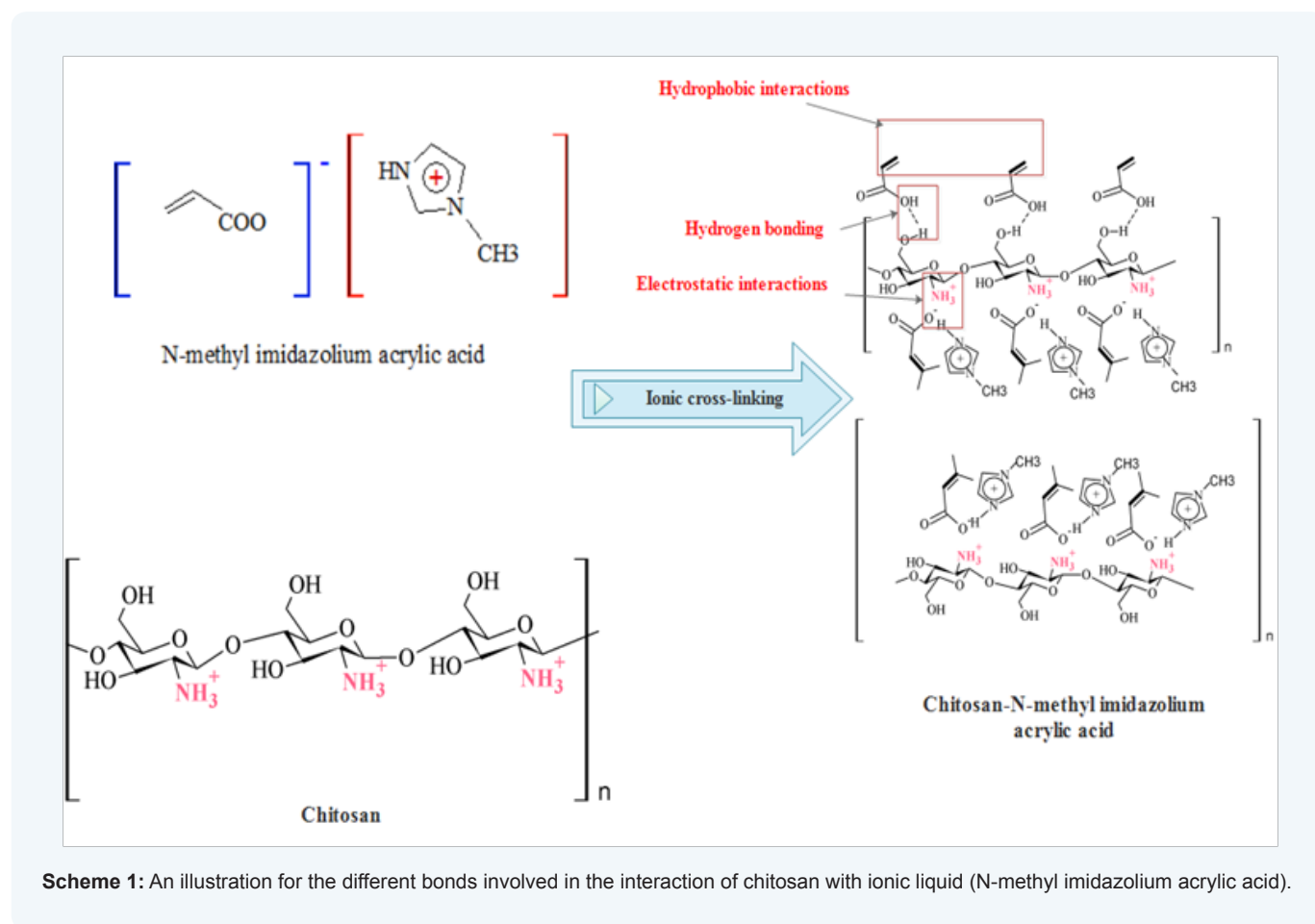
## Materials and Methods

### Materials

Chitosan (low molecular weight, inherent viscosity 30,000 cP, Sigma-Aldrich, USA), acrylic acid, N-methyl imidazole (Sigma-Aldrich, ON, CA), iron (II) sulfate heptahydrate ( $\text{FeSO}_4 \cdot 7\text{H}_2\text{O}$ ), ethanol, diethyl ether and sodium hydroxide (Na OH) (VWR, ON, CA).

### Ionic liquid- $\text{Fe}_3\text{O}_4$ core / chitosan shell magnetic hydrogel

**Synthesis of CS-MIAA Hydrogels:** N-methyl imidazolium acrylic acid (MIAA) was synthesized following the protocol reported Ohno et al. [20]. Chitosan stock gel was first prepared at 2.5 wt% in 0.1M hydrochloric acid and the pH was adjusted to 6.5 by drop wise addition of 1M sodium hydroxide. Chitosan-ionic liquid hydrogel was prepared by drop wise addition of equal volumes of 8, 15, 18, 22 and 30 mmol of MIAA into 0.2 wt% chitosan solution (pH = 6.5). The mixture was then placed in a rotary shaker at 300 rpm for 24 h in order to obtain the hydrated gel. The chemical structures of chitosan, MIAA and chitosan-ionic liquid hydrogel were illustrated in Scheme 1.



**Synthesis of ionic liquid-Fe<sub>3</sub>O<sub>4</sub> core / chitosan shell magnetic hydrogel:** Ionic liquid-chitosan hydrogel was added into a solution of iron precursor (1.396 g FeSO<sub>4</sub>·7H<sub>2</sub>O), sonicated for 30 min in an ultrasonic bath at 25 °C. The pH of the medium was gradually increased by drop wise addition of ammonium hydroxide (NH<sub>4</sub>OH, pH = 13). The reaction temperature was elevated to 90 °C and mixing was continued for 90 min. The excess ammonium hydroxide was removed and the obtained magnetic hydrogels were separated and freeze dried for solid state analysis (Free Zone 12 Liter Console Freeze Dry Systems, Labconco, USA).

**Characterization of Fe<sub>3</sub>O<sub>4</sub> magnetic nanoparticles and freeze dried ionic liquid-Fe<sub>3</sub>O<sub>4</sub> core / chitosan shell magnetic hydrogel**

Particles diameters were analyzed using dynamic light scattering (DLS) technique (Zeta sizer, 300 HSA, Malvern, UK). The analysis was performed at a scattering angle of 90° and at a temperature of 20° C. The surface morphology of magnetic nanoparticles was investigated using scanning electron microscopy (SEM) (Hitachi High-Technologies GmbH, Germany). The samples were prepared on aluminum stabs, coated with gold and measured at an accelerating voltage of 20 kV coupled with energy dispersive (EDX) for elemental analysis. FT-IR spectra were measured on a Nicolet, Magna-550 spectrometer (Scientific Equipment Source, Ontario, CA). For sample preparation on FT-IR, magnetic powders were mixed with potassium bromide (KBr) and pressed for measurement.

**In-vitro drug release of progesterone from ionic liquid-Fe<sub>3</sub>O<sub>4</sub> core / chitosan shell magnetic hydrogel**

The drug release mechanism of magnetic ionic liquid-Fe<sub>3</sub>O<sub>4</sub> core / chitosan shell loaded samples was investigated. Each experiment contained 20 mg of progesterone loaded magnetic hydrogels placed in a Pur-A-Lyzerdialysis kit (12,000 kDa, Sigma Aldrich, Canada) exposed to 60 ml buffer solution in the

external compartment (pH = 7.4). The amount of progesterone released was quantified using UV-Vis spectrophotometer at 254 nm maximum wavelength. All drug release experiments were repeated in triplicates. In order to investigate the effect of pH on the release profile of progesterone, two different sets of buffer solutions were examined (pH = 6.5 and 7.4) at 37 °C. The dependence of release kinetics on magnetic field was studied by applying a constant magnetic field of intensity 33MGoe.

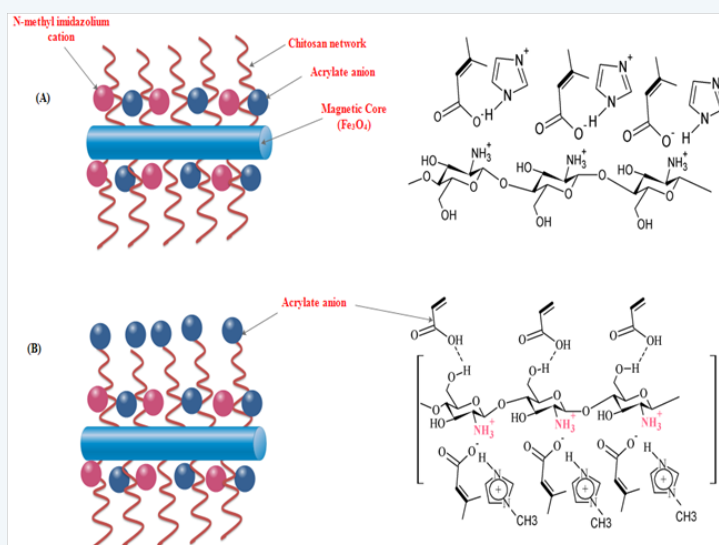
**Swelling test**

The swelling behavior of CS- and CS-MIAA-coated magnetic nanorods was evaluated using gravimetric technique. A premeasured amount of freeze dried hydrogel (100 mg, W<sub>1</sub>) was first dispersed in 5 ml distilled water at 37 °C. At a predetermined time interval, hydrogel samples were dried by pressing between two filter papers and then weighed (W<sub>2</sub>). The swelling of different samples was determined at different time points. The percentage swelling (water uptake) was calculated based on Equation 1. The capacity of water absorption was examined at different pH (6.5 and 7.4), with and without the application of a constant magnetic field.

$$\% \text{ Swelling Index (SI)} = \frac{W_2 - W_1}{W_1} \times 100 \dots\dots\dots (1)$$

**In-vitro cytotoxicity**

Metabolic activity of C3H 10T1/2 cells was determined by a tetrazolium-based colorimetric MTT assay [21]. The ability of the cells to reduce 3-[4,5-dimethylthiazol-2-yl]-2,5 diphenyltetrazolium bromide (MTT) indicates their metabolic activity. Cells were pre-cultured for 24 hr at seeding density 8,000 cells/well (96-well plate) and then treated using differential beads at different concentrations. MTT absorbance values were measured after 48 h of culture. Data are expressed as mean ± standard error for experiments conducted in triplicate.



**Scheme 2:** A presentation of the network configuration of chitosan-N-methyl imidazolium acrylate at different concentration regimes of ionic cross-linker: (A) 8 mmol N-methyl imidazolium acrylate and (B) 30 mmol N-methyl imidazolium acrylate.

## Results and Discussion

Ionic liquid-Fe<sub>3</sub>O<sub>4</sub> core / chitosan shell magnetic hydrogels were successfully synthesized with variable concentrations of ionic liquid. The possibility of controlled macroscopic properties and tunable drug release were investigated based on the network structure of hydrogels. The proposed chemical structure for the synthesized hydrogel is illustrated in Scheme 1 and Scheme 2. Based on the presented structures, either intra- or inter-molecular cross-links could be introduced into the chitosan backbone depending on the molar concentration of ionic cross-linker. Consequently, the change in the water absorption capacity and the internal geometry of chitosan network could be accomplished.

### Morphology of magnetic ionic liquid-Fe<sub>3</sub>O<sub>4</sub> core / chitosan shell magnetic nanoparticles

FESEM images of magnetic nanorods coated with 15 mmol of ionic cross-linker are presented in Figure 1. The images indicate the formation of nanorods; with diameters < 30 nm and a length of approximately 140 nm. Increasing the concentration

of ionic cross-linker from 8 to 30 mmol resulted in a remarkable capability of varying the size of magnetic nanorods. Table 1 illustrates the effect of formulation variables on the particle size and polydispersity index of magnetic nanorods. The illustrated data agrees well with previous studies that demonstrate the effect of ionic liquid on changing the structural organization of nanomaterial surface as well as reshaping of nanoparticles [22].

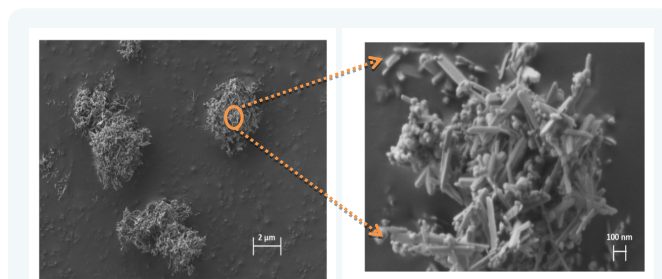


**Figure 1:** FE-SEM images of the ionic liquid-Fe<sub>3</sub>O<sub>4</sub> core @ chitosan magnetic nanoparticles.

**Table 1:** Effect of formulation parameters on the particle size, polydispersity index, drug loading and encapsulation efficiency of CS-MIAA coated magnetic nanoparticles.

Drug input (mg)	Chitosan concentration (mg/ml)	MIAA concentration (mmol)	Particle size (nm)	Polydispersity index	Drug loading (%)
5	2	8	23.2 ± 1.98	0.19 ± 0.25	30 ± 2.75
10	2	8	23.2 ± 1.98	0.19 ± 0.25	34.5 ± 3.12
10	2	15	21.8 ± 2.09	0.17 ± 0.03	36 ± 2.95
10	2	18	25.5 ± 1.56	0.25 ± 0.03	32.5 ± 3.01
10	2	22	28.3 ± 2.54	0.41 ± 0.04	35 ± 3.42
10	2	30	32.4 ± 2.95	0.46 ± 0.06	37.5 ± 2.85

### Chemical composition of ionic liquid-Fe<sub>3</sub>O<sub>4</sub> core / chitosan shell architecture

The FTIR spectra (Figure 2) of ionic liquid-Fe<sub>3</sub>O<sub>4</sub> core / chitosan shell magnetic hydrogels revealed the interaction between chitosan and the imidazolium ring of ionic cross-linker (N-methyl imidazolium acrylic acid, MIAA). The appearance of peaks corresponding to the carboxylate stretching vibrations; indicates the presence of acrylic acid anion on the hydrogels. The typical bending vibration for chitosan amine group (NH<sub>2</sub>), which is centered at 1545 cm<sup>-1</sup>, moved to the peaks at 1593 and 1616 cm<sup>-1</sup>. This shift was due to the asymmetric and symmetric vibrations of NH<sub>3</sub><sup>+</sup> group; which indicates the electrostatic interaction between the carboxylate group of acrylic acid moiety in MIAA ionic liquid and the amine group of chitosan, CS, (Scheme 1). The peak at 635 cm<sup>-1</sup> is assigned for Fe-O group. The broad band observed at 3400 cm<sup>-1</sup> for the uncoated magnetite sample can be referred to the -OH group. The symmetric CH<sub>2</sub> stretch can be allocated at 2847 cm<sup>-1</sup> for CS- and CS-MIAA coated magnetic nanoparticles.

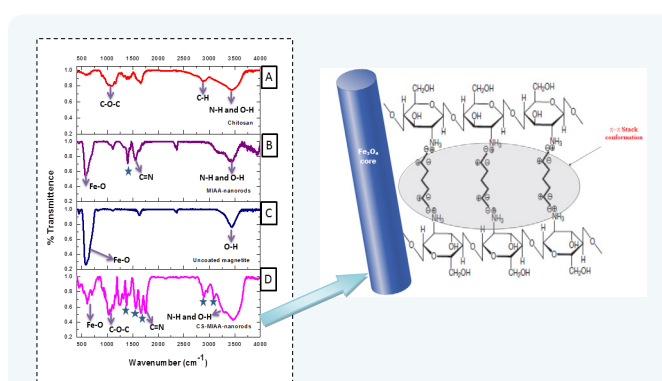


**Figure 2:** FTIR spectra for chitosan (A), MIAA-coated magnetic nanorods (B), uncoated magnetite (C) and chitosan-ionic liquid-coated magnetic nanorods (D). The peaks marked with asterisks correspond to π-π stacking of imidazole rings.

The absorption band at 1070 cm<sup>-1</sup> resulted from the stretching vibration of the C-O bond in the CH<sub>2</sub>-OH group for both CS- and CS-MIAA coated samples.

In addition, the proposed  $\pi$ - $\pi$  stack interaction of imidazolium ring demonstrated in Scheme 1 was further confirmed by FTIR spectra. The change of the peak position assigned for the C-N stretching vibration of imidazolium ring (marked with an asterisk in Figure 2B) towards lower wave numbers. The  $\pi$ - $\pi$  stacking can also be examined by the change in the C-H stretching vibration of imidazolium ring at 2880-3160  $\text{cm}^{-1}$  (Figures 2B and 2D). The peak broadening together with the shift in the absorption peaks towards lower wavenumbers probably originating from the  $\pi$ - $\pi$  stack interactions of positively charged imidazole, which decreased the electron density of the C-H bond of the ring. The appearance of three strong absorption peaks in the spectrum (Figure 2D) additionally confirms the imidazolium packing proposed in Scheme 2.

### Kinetic swelling study of ionic liquid- $\text{Fe}_3\text{O}_4$ core / chitosan shell magnetic hydrogels

Figures 3-5 demonstrate the results of a kinetic study of the

water absorption behavior of ionic liquid- $\text{Fe}_3\text{O}_4$  core / chitosan shell magnetic hydrogels. The calculated swelling index varies from  $100 \pm 4.51\%$  to  $62 \pm 4.65\%$  for different hydrogel samples examined after 60 min (Figure 3).

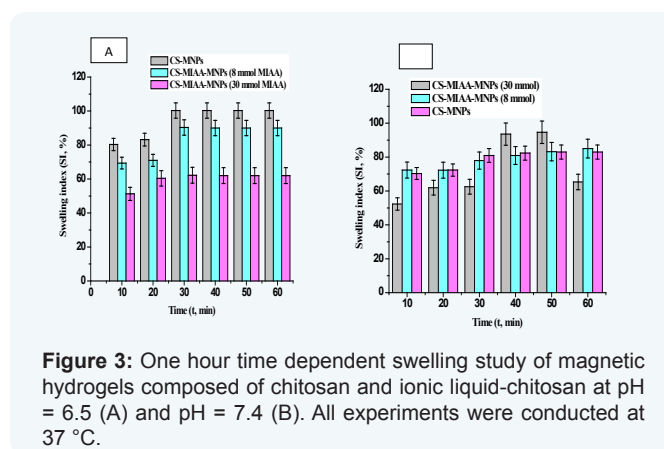


**Figure 3:** One hour time dependent swelling study of magnetic hydrogels composed of chitosan and ionic liquid-chitosan at pH = 6.5 (A) and pH = 7.4 (B). All experiments were conducted at 37 °C.

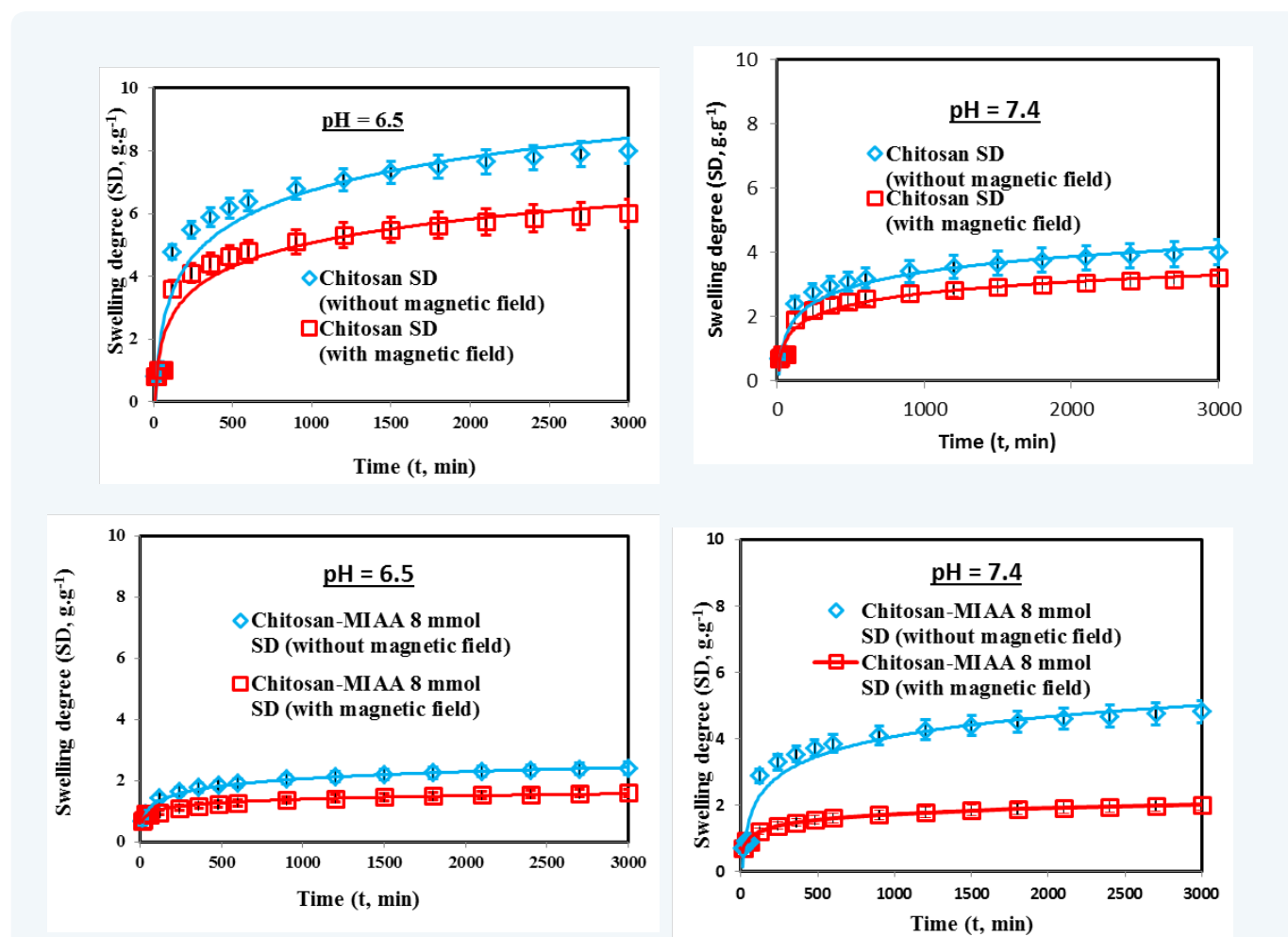


**Figure 4:** Time dependent swelling degree ( $\text{g.g}^{-1}$ ) of magnetic hydrogels composed of chitosan (A and B) and chitosan-8 mmol N-methyl imidazolium acrylic acid, MIAA, (C and D). The experiments were conducted with and without an external magnetic field application.

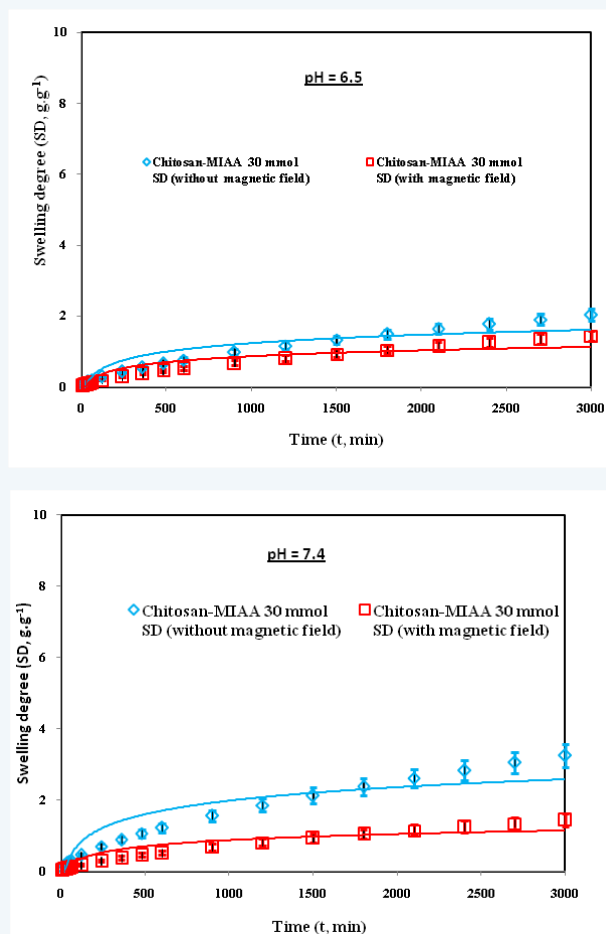


**Figure 5:** Time dependent swelling degree (g.g<sup>-1</sup>) of magnetic hydrogels composed of chitosan-8 mmol N-methyl imidazolium acrylic acid, MIAA, at pH 6.5 (A) and pH 7.4 (B). The experiments were conducted with and without an external magnetic field application.

Non cross-linked Fe<sub>3</sub>O<sub>4</sub> core / chitosan shell samples showed the highest swelling index value (SI = 83.21 % ± 3.74 at pH = 6.5, after 20 min). Moreover, changes in the reacting ionic cross-linker concentrations significantly affected the swelling behaviour of the prepared hydrogels.

The water absorption capacities of the obtained hydrogels were quantified in either distilled water (pH=6.5) or phosphate buffer saline (PBS, pH= 7.4) in order to simulate the physiological environment. Figure 4 and Figure 5 show a two-days-time-dependent swelling profile of ionic liquid-Fe<sub>3</sub>O<sub>4</sub> core / chitosan shell magnetic hydrogels with and without the application of a constant magnetic field. Magnetic hydrogels samples prepared with 8 and 30mmol of ionic cross-linker demonstrated a magnetic field responsive swelling behaviour. A more profound effect was observed at pH = 7.4, the swelling degree was decreased from 4.8 % to 2.0 % for the 8 mmol ionic liquid-Fe<sub>3</sub>O<sub>4</sub> core / chitosan shell magnetic sample, with applying a constant magnetic field (Figure 5). At high concentration of ionic cross-linker (30 mmol,

Figure 6), the hydrogels swelling profile showed less marked changes in response to an applied magnetic field. This could be attributed to the higher density of polymer chains; which makes the network expansion more difficult. The mechanism of hydrogel swelling is actually driven by the spontaneous mixing of chitosan network with water; which results from coupling the effect of hydrophobic interactions among the polymeric chain and the electrostatic interactions between the ionic moieties. Therefore, in order to understand the swelling behaviour of ionic liquid-Fe<sub>3</sub>O<sub>4</sub> core / chitosan shell magnetic hydrogels, it is important to investigate the molecular organization of chitosan network. Based on the proposed molecular structure presented in Scheme 1 and starting with a fixed amount of chitosan, differences in the network cross-linking density were most likely attributed to the differences in ionic liquid concentrations. The change in chitosan molecular arrangements will be mainly reflected on changing the molecular weight, molecular flexibility, hydrodynamic diameter of the produced polymeric network. Furthermore, the non-reacted amine group of chitosan should be also considered. The medium pH was also shown to play an important role in the swelling of hydrogel. The interesting behavior of chitosan could be referred to its poly-cationic nature. Native chitosan has a pKa value ranging from 6.2 to 7, therefore, the terminal amine groups are protonated at pH = 6.5 and neutralized at pH = 7.4. In case of distilled water, the swelling index of ionic liquid cross-linked chitosan was slightly decreased. This could be attributed to the fact that the neutralization of the positive charge of NH<sub>2</sub>- groups with the negatively charged acrylate moieties that are arranged along the chitosan network. On the other hand, at pH=7.4, the NH<sub>2</sub>-groups are neutralized, consequently the swelling index is slightly increased due to the electrostatic repulsive forces between the negatively charged acrylate groups. The data presented in Figures 3-5 indicate that the swelling behavior of ionic liquid-Fe<sub>3</sub>O<sub>4</sub> core / chitosan shell magnetic hydrogels are controlled mainly by the following parameters: (I) architecture of chitosan network; which is based on the concentration of ionic cross-linker, (II) pH of the swelling medium; which affects the occurrence of neutral of cationic amine termination of chitosan backbone, and (III) application of a constant magnetic field.

### Effect of pH, cross-linker concentration and application of magnetic field on the release pattern of progesterone from ionic liquid-Fe<sub>3</sub>O<sub>4</sub> core / chitosan shell magnetic hydrogels

Figures 6-8 show the effect of different formulation and release medium variables on the release profile of progesterone from different magnetic hydrogels. The effect of pH is highlighted in Figure 6 for the magnetic hydrogels composed of chitosan and chitosan-N-methyl imidazolium acrylic acid (8 mmol). For the magnetic hydrogels coated with chitosan, less prolonged release duration together with a faster release rate was observed. However, incorporating ionic cross-linker into the hydrogel network resulted in an extended release profile for 10 days (hydrogel sample composed of 8 mmol of ionic cross-linker).

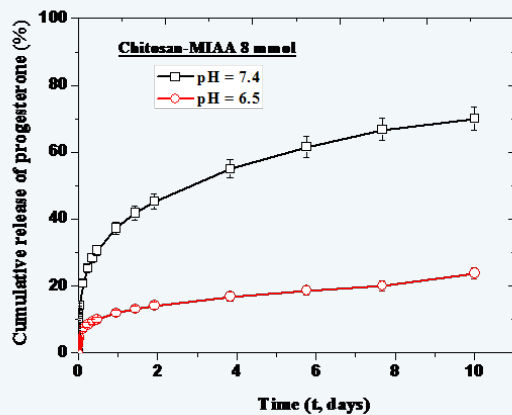
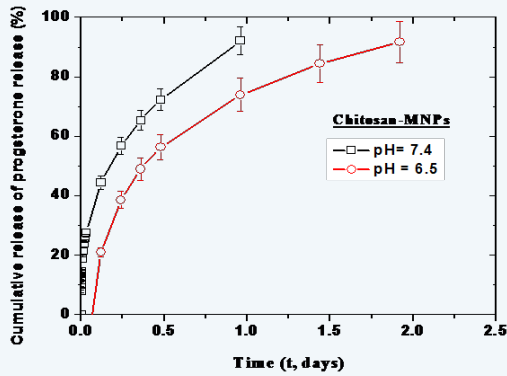


**Figure 6:** In vitro release profile of progesterone from magnetic hydrogels composed of chitosan (A) and chitosan-N-methyl imidazolium acrylic acid 8 mmol (B).

The experiments were conducted at pH 6.5 and pH 7.4.

The release rate of progesterone from magnetic hydrogels was significantly controlled with the concentration of ionic cross-linker and the pH of release medium (Figures 6 and 7). Less significant effect of the pH was observed for the hydrogels composed of 30 mmol ionic cross-linker concentration. Moreover, investigating the effect of magnetic field on the release profile revealed a significant difference for the hydrogels composed of 8, 15 and 18 mmol of ionic cross-linker. Results for the 18 mmol N-methyl imidazolium acrylic acid were exemplarily presented in Figure 7B. Absence of significant effect of magnetic field application for the samples composed of magnetic Fe<sub>3</sub>O<sub>4</sub> core (Figure 7A) and 30 mmol of N-methyl imidazolium acrylic acid (results are not shown).

The effect of magnetic field application on the release profile of progesterone from magnetic core and magnetic coated nanoparticles was illustrated in Figure 8. Generally, progesterone showed more controlled release profile with a significantly less initial burst effect upon exposure to an externally applied magnetic field. A more prominent effect has been observed for the magnetic nanoparticles coated with chitosan-18 mmol ionic liquid composite (Figure 8B).

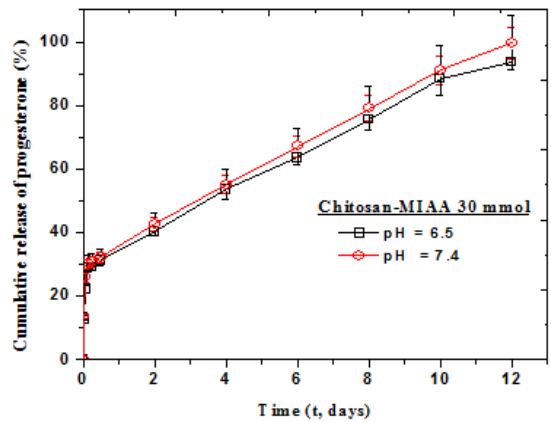
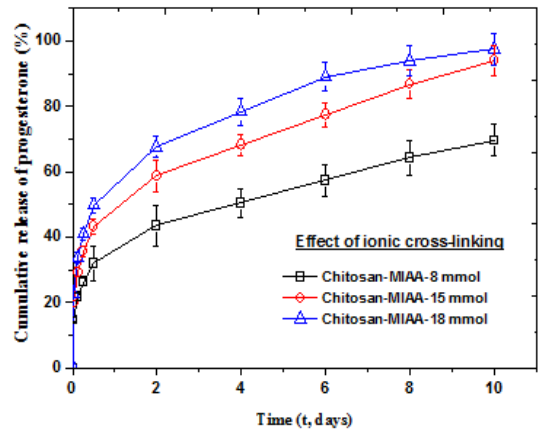


**Figure 7:** Effect of ionic cross-linker concentration on the release profile of progesterone from magnetic hydrogels composed of chitosan-N-methyl imidazolium acrylic acid 8, 15 and 18 mmol (A), 30 mmol (B).

Absence of significant effect of pH on the release profile examined at 30 mmol ionic cross-linker

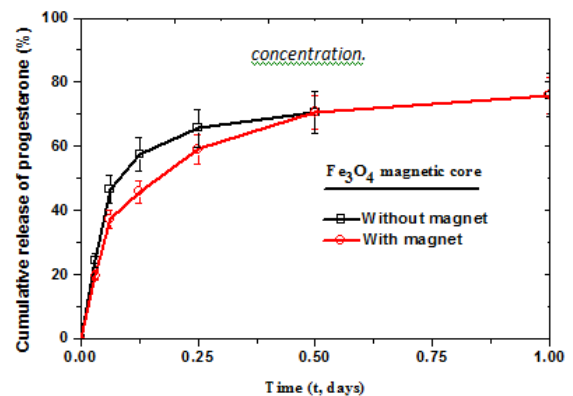


**Figure 8:** Effect of magnetic field application on the release profile of progesterone from magnetic core Fe<sub>3</sub>O<sub>4</sub> (A) and magnetic hydrogels composed of chitosan-N-methyl imidazolium acrylic acid 18 mmol (B).

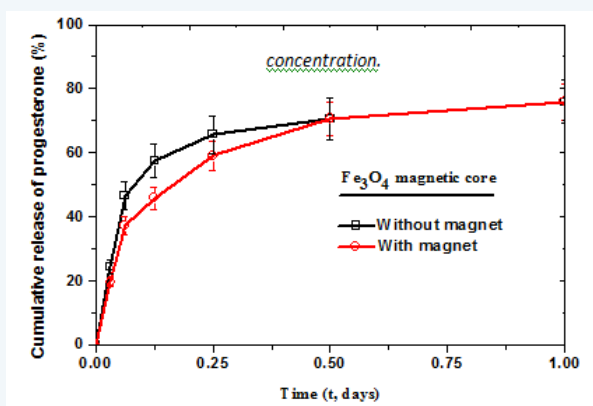


**Figure 8:** Effect of magnetic field application on the release profile of progesterone from magnetic core Fe<sub>3</sub>O<sub>4</sub> (A) and magnetic hydrogels composed of chitosan-N-methyl imidazolium acrylic acid 18 mmol (B).

**In-vitro cytotoxicity of ionic liquid-Fe<sub>3</sub>O<sub>4</sub> core / chitosan shell magnetic nanoparticles**

The *in-vitro* cytotoxicity of the synthesized magnetic nanoparticles was assessed by performing MTT assay on C3H 10T1/2. The cells were pre-cultured for 24 h with different concentrations of magnetic nanoparticles including the non-cross-linked and the ionic-cross-linked samples. The assay shows that chitosan and the ionic cross-linker, up to 30 mmol concentration, are well tolerated with the cells (Figure 9).

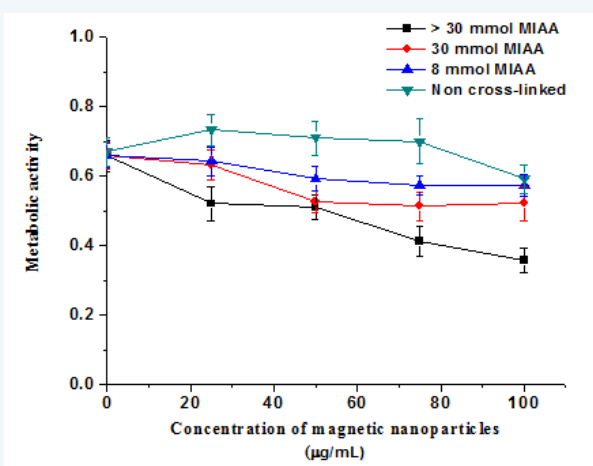


**Figure 9:** In vitro cytotoxicity study of the synthesized ionic liquid-Fe<sub>3</sub>O<sub>4</sub> core @ chitosan-shell magnetic nanoparticles. The graph presents the metabolic activity versus the concentration of magnetic nanoparticles.

The results present the mean values ± SE.

**Discussion**

**Drug encapsulation and release behavior of progesterone from ionic liquid-Fe<sub>3</sub>O<sub>4</sub> core / chitosan shell magnetic hydrogels**

Based on preliminary experiments, 10 mg of progesterone was selected as the amount of drug input for all examined samples.

Changing the concentration of ionic cross-linker in the composite resulted in increasing the drug encapsulation efficiencies from 69 ± 5.42 % to 75 ± 5.7 %. The highest percentages of drug loading and encapsulation efficiencies occurred for the sample functionalized with 30 mmol of MIAA (Table 1). Further increase in ionic cross-linker concentration decreased both the drug loading and encapsulation efficiency; because of the inability of progesterone to penetrate through the cross-linked network structure of chitosan. Analysis of progesterone release kinetics from ionic liquid-Fe<sub>3</sub>O<sub>4</sub> core / chitosan shell magnetic hydrogels was performed using Peppas model [19]:

$$\frac{M_t}{M_\infty} = kt^n \dots\dots\dots (2)$$

where  $M_t / M_\infty$  is the fraction of drug released at time (t), k is the release rate constant and n is the diffusional exponent; that depends on the mechanism of drug release and the shape of drug delivery system (Table 2). Investigating the mechanistic data based on mathematical modeling of different release profiles indicates that the release mechanism for the samples prepared with ionic cross-linker (concentrations up to 22mmol) is Fickian diffusion. Increasing the concentration of MIAA produced drug delivery systems with an anomalous release mechanism (coupled transport). A more revealing understanding of the drug release from swelling matrices was summarized in Table 3.

**Mathematical modeling of progesterone release from ionic liquid-Fe<sub>3</sub>O<sub>4</sub> core / chitosan shell magnetic hydrogels**

By fitting the drug release data to the model (Equation 3) proposed by Peppas and Sahlin [23], a quantitative understanding of the diffusion and relaxation mechanisms can be attained.

$$\frac{M_t}{M_\infty} = k_1t^m + k_2t^{2m} \dots\dots\dots (3)$$

Where, the term ( $k_1t^m$ ) represents the Fickian diffusion contribution (FD) and the second term ( $k_2t^{2m}$ ) represents the relaxation contribution (R) on the polymeric matrix. The ratio of the relaxation and diffusion can be presented as:

$$\frac{R}{F_D} = \left[ \frac{K_1}{K_2} \right] \times t^m \dots\dots\dots (4)$$

The release data were analyzed based on Equations 3 and 4. Figure 10 shows the calculated  $R/F_D$  versus the fractions of progesterone released over the 14 days. With increasing the concentration of MIAA form 8 to 30 mmol, the ratio  $R/F_D$  remains very low; indicating that the drug release mechanism is almost diffusion-controlled. Further increase in the weight fractions of MIAA is associated with an increase in the calculated  $R/F_D$  as a result of the increased resistance of drug diffusion. The results presented revealed the possibility of shifting from Fickian to anomalous diffusion upon changing the polymeric composite



structure (Figure 10 and Scheme 3). The plotted release data were mathematically modeled using Peppas equations. The Akaike Information Criterion (AIC), presented in Equation 5, has been applied for selecting the optimum model of drug release.

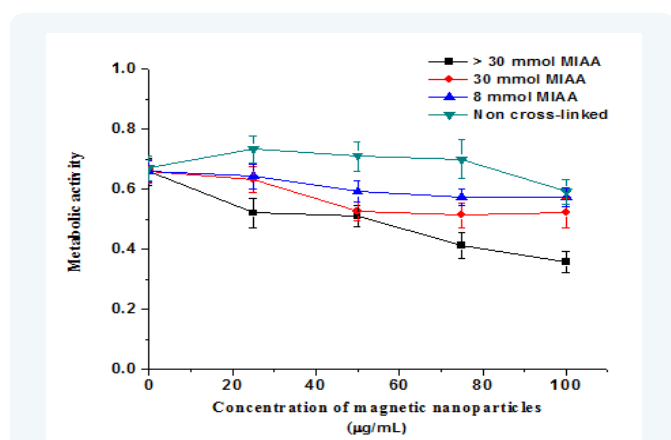
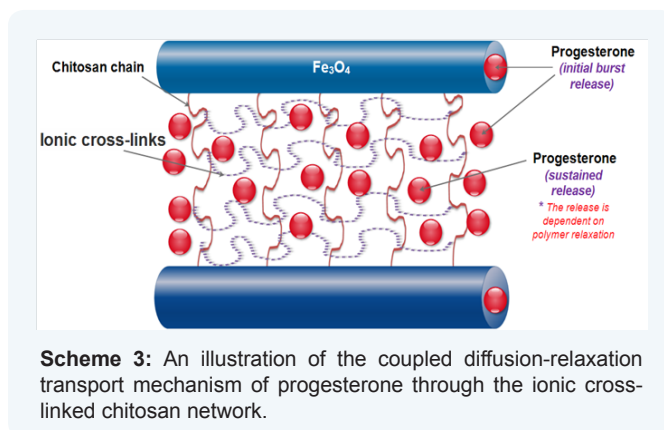


**Figure 10:** The calculated relaxation / diffusion (R/FD) for the release of progesterone from ionic liquid-Fe<sub>3</sub>O<sub>4</sub> core @ chitosan shell magnetic hydrogels composed of 18, 22 and 30 mmol of N-methyl imidazolium acrylic acid.



**Scheme 3:** An illustration of the coupled diffusion-relaxation transport mechanism of progesterone through the ionic cross-linked chitosan network.

**Table 2:** Prediction of the diffusion mechanism based on the calculated release exponent values.

Drug release mechanism	Release exponent (n)
Case I transport (Fickian diffusion)	n ≤ 0.5
Anomalous diffusion (non Fickian or coupled diffusion)	0.5 < n < 1.0
Case II transport (Zero order)	n = 1.0

**Table 3:** Summary of release kinetics data obtained by mathematical curve fitting with Peppas-Sahlin model with a calculated goodness of model fit data (R<sup>2</sup>, WSS and AIC).

Sample	K <sub>1</sub>	K <sub>2</sub>	m	T50 (days)	R <sup>2</sup>	WSS	AIC
8 mmol MIAA	27.32 ± 1.33	9.65 ± 0.47	0.204 ± 0.054	3.173 ± 0.601	0.99	15.26	33.25
15 mmol MIAA	36.88 ± 1.79	13.03 ± 0.633	0.206 ± 0.0389	1.022 ± 0.232	0.99	27.82	39.26
18 mmol MIAA	58.24 ± 7.29	4.38 ± 0.99	0.245 ± 0.042	0.56 ± 0.136	0.99	14.68	32.87
22 mmol MIAA	26.55 ± 2.13	10.98 ± 0.88	0.182 ± 0.039	3.47 ± 0.31	0.96	264.75	89.68
30 mmol MIAA	28.24 ± 1.11	12.28 ± 0.58	0.238 ± 0.055	1.91 ± 0.28	0.95	387.05	77.5

$$AIC = n \cdot \ln(WSS) + 2 \cdot p \dots\dots\dots (5)$$

Where, n is the number of data points, WSS is the weighed sum of squares and p is the number of parameters in the model. From the definition described in Equation 5, the AIC is dependent on the magnitude of data as well as the number of data points. The WSS and AIC values for the CS-Fe<sub>3</sub>O<sub>4</sub> magnetic nanoparticles prepared at different concentration of ionic liquid were presented in Table 3.

In this study, we compared different models for the best fit with progesterone release data from magnetic nanorods. Peppas model was assigned for the lowest AIC for our experimental release data; therefore, it is the best fitted for drug modeling. The presented data confirms that high concentrations of ionic liquid results in more entanglement of chitosan chains; decreasing the drug diffusion coefficient due to relaxation of the polymer [24]. The release rate and diffusion exponent could be directly linked to the cross-link density of polymeric networks [25].

### An investigation on the water transport mechanism through ionic liquid-Fe<sub>3</sub>O<sub>4</sub> core / chitosan shell magnetic hydrogels

The parameters of swelling kinetics of different magnetic hydrogels are shown in Table S-1 and Table S-2. The swelling mechanism of chitosan-coated Fe<sub>3</sub>O<sub>4</sub> and ionic liquid-Fe<sub>3</sub>O<sub>4</sub> core / chitosan shell magnetic hydrogels (8 mmol N-methyl imidazolium acrylic acid) were all described with Fickian transport mechanism (n < 0.45). The mechanism of water transport through the magnetic hydrogels is independent of the applied magnetic field or the pH. However, the swelling rate parameter k is significantly affected by the pH for the chitosan-coated Fe<sub>3</sub>O<sub>4</sub> samples. A less significant effect was observed for the samples composed of 8 mmol N-methyl imidazolium acrylic acid. A slower swelling rate was observed when the concentration of ionic cross-linker was increased to 30 mmol (TableS-2). At both values of examined pH, the swelling data fitted well to the anomalous mechanism (0.45 < n < 0.89). The observed data indicates the coupling of

Fickian diffusion and polymer relaxation mechanisms. The values of k indicated a more controlled swelling upon increasing the concentration of ionic cross-linker; which explains the more controlled drug release profile.

**Table S 1:** Effect of magnetic field on the Kinetic parameters [(release rate constant, k) and (release exponent, n)] of Fe3O4-core-chitosan-shell at different pH.

Sample	Adjusted R <sup>2</sup>	Release rate constant (k, day <sup>-1</sup> )	p	Release exponent n	p	Transport mechanism
Chitosan (pH = 6.5, no magnet)	0.8627	0.7201	0.0037	0.3138	< 0.0001	Fickian transport
Chitosan (pH = 6.5, with magnet)	0.8804	0.6159	0.001	0.2963	< 0.0001	Fickian transport
Chitosan (pH = 7.4, no magnet)	0.8974	0.4676	0.0002	0.279	< 0.0001	Fickian transport
Chitosan (pH = 7.4, with magnet)	0.9487	0.439	< 0.0001	0.2575	< 0.0001	Fickian transport

**Table S 2:** Effect of magnetic field on the Kinetic parameters [(release rate constant, k) and (release exponent, n)] of ionic cross-linked Fe3O4-core-chitosan-shell at different pH.

Sample	Adjusted R <sup>2</sup>	Release rate constant (k, day <sup>-1</sup> )	p	Release exponent n	p	Transport mechanism
CS-MIAA (8 mmol, pH = 6.5, no magnet)	0.9611	0.4542	< 0.0001	0.2143	< 0.0001	Fickian transport
CS-MIAA (8 mmol, pH = 6.5, with magnet)	0.9732	0.5023	< 0.0001	0.1452	< 0.0001	Fickian transport
CS-MIAA (8 mmol, pH = 7.4, no magnet)	0.8885	0.5212	0.0005	0.2889	< 0.0001	Fickian transport
CS-MIAA (8 mmol, pH = 7.4, with magnet)	0.9827	0.4667	< 0.0001	0.1859	< 0.0001	Fickian transport
CS-MIAA (30 mmol, pH = 6.5, no magnet)	0.9802	0.0158	< 0.0001	0.6072	< 0.0001	Non-Fickian transport
CS-MIAA (30 mmol, pH = 6.5, with magnet)	0.9701	0.0097	< 0.0001	0.6251	< 0.0001	Non-Fickian transport
CS-MIAA (30 mmol, pH = 7.4, no magnet)	0.9865	0.0158	< 0.0001	0.607	< 0.0001	Non-Fickian transport
CS-MIAA (30 mmol, pH = 7.4, with magnet)	0.9524	0.0097	< 0.0001	0.625	< 0.0001	Non-Fickian transport

## Conclusions

Ionic liquid-Fe<sub>3</sub>O<sub>4</sub> core / chitosan shell magnetic hydrogels were successfully synthesized. Control of progesterone initial burst effect was achieved by increasing the concentration of ionic liquid in the composite. Adjustment of the swelling kinetics of chitosan helped in controlling the drug release rate. The drug release profile was mathematically modeled and the transport through the magnetic hydrogels was controlled by both diffusion and polymer relaxation processes. A relationship was constructed between the coating composition and the release mechanism of progesterone with an insight on the chemical configuration of the system. The presented method for monitoring magnetic swelling demonstrates the effectiveness of our proposed hydrogels in terms of magnetic localization and controlled hormonal therapy.

**Acknowledgement:** The authors acknowledge the financial assistance received from the Natural Sciences and Engineering Research Council of Canada (NSERC), Ontario Graduate Scholarship (OGS) and the Faculty of Engineering of the University

of Western Ontario to conduct this research.

## References

- Seliktar D (2012) Designing cell-compatible hydrogels for biomedical applications. *Science* 336(6085): 1124-1128.
- Bhattarai N, Gunn J, Zhang M (2010) Chitosan-based hydrogels for controlled, localized drug delivery, *Adv Drug Deliv Rev* 62 (1): 83-99.
- Censi R, Di Martino P, Vermonden T, Hennink WE (2012) Hydrogels for protein delivery in tissue engineering. *J Control Release* 161(2): 680-692.
- Wu Y, Wu S, Hou L, Wei W, Zhou M, et al. (2012) Novel thermal-sensitive hydrogel enhances both humoral and cell-mediated immune responses by intranasal vaccine delivery, *Eur J Pharm Biopharm* 81(3): 486-497.
- Chun KW, Lee JB, Kim SH, Park TG (2005) Controlled release of plasmid DNA from photo-cross-linked pluronic hydrogels. *Biomaterials* 26(16): 3319-3326.
- Chiemi Okaa, Kazunori Ushimarua, Nanao Horiishib, Takeharu Tsugea, Yoshitaka Kitamoto (2015) Core-shell composite particles composed of biodegradable polymer particles and magnetic iron

- oxide nanoparticles for targeted drug delivery. *Journal of Magnetism and Magnetic Materials* 381: 278-284.
7. Fuchigami T, Kawamura R, Kitamoto Y, Nakagawa M, Namiki Y (2011) Ferromagnetic FePt-nanoparticles/polycation hybrid capsules designed for a magnetically guided drug delivery system. *Langmuir* 27(6): 2923-2928.
  8. M Abe, N Nishioc, M Hatakeyam, N Hanyud, T Tanaka, et al. (2009) Nakagawa Preparation and medical application of magnetic beads conjugated with bioactive molecules. *Journal of Magnetism and Magnetic Materials* 321(7): 645-649.
  9. Bardajee GR, Hooshyar Z (2014) One-pot synthesis of biocompatible superparamagnetic iron oxide nanoparticles/hydrogel based on salep: Characterization and drug delivery. *Carbohydr Polym* 101: 741-751.
  10. Kowalczyk A, Fau M, Karbarz M, Donten M, Stojek Z, et al. (2014) Hydrogel with chains functionalized with carboxyl groups as universal 3D platform in DNA biosensors. *Biosens Bioelectron* 54: 222-228.
  11. YA. Ismail, J.G. Martínez, A.S. Al Harrasi, S.J. Kim, T.F. Otero, Sensing characteristics of a conducting polymer/hydrogel hybrid microfiber artificial muscle, *Sensors and Actuators, B: Chemical*, 160 (2011) 1180-1190.
  12. Tronci G, Ajiro H, Russell SJ, Wood DJ, Akashi M (2014) Tunable drug-loading capability of chitosan hydrogels with varied network architectures. *Acta Biomater* 10(2): 821-830.
  13. Schillemans JP, Verheyen E, Barendregt A, Hennink WE, Van Nostrum CF (2011) Anionic and cationic dextran hydrogels for post-loading and release of proteins. *J Control Release* 150(3): 266-271.
  14. Kiser PF, Wilson G, Needham D (1998) A synthetic mimic of the secretory granule for drug delivery. *Nature* 394(6692): 459-462.
  15. Iskakov RM, Kikuchi A, Okano T (2002) Time-programmed pulsatile release of dextran from calcium-alginate gel beads coated with carboxy-n-propylacrylamide copolymers. *J Control Release* 80(1-3): 57-68.
  16. Ogomi D, Serizawa T, Akashi M (2005) Controlled release based on the dissolution of a calcium carbonate layer deposited on hydrogels. *J Control Release* 103(2): 315-323.
  17. Takemoto Y, Ajiro H, Asoh T, Akashi M (2010) Fabrication of Surface-Modified Hydrogels with Polyion Complex for Controlled Release. *Chemistry of Materials* 22: 2923-2929.
  18. Martínez-Ruvalcaba A, Sánchez-Díaz JC, Becerra F, Cruz-Barba LE, González-Álvarez A (2009) Swelling characterization and drug delivery kinetics of polyacrylamide-co-itaconic acid/chitosan hydrogels. *Express Polymer Letters* 3: 25-32.
  19. Ritger PL, Peppas NA (1987) A simple equation for description of solute release I. Fickian and non-fickian release from non-swelling devices in the form of slabs, spheres, cylinders or discs. *Journal of Controlled Release* 5(1): 23-36.
  20. Ohno H, Yoshizawa M, Ogihara W (2004) Development of new class of ion conductive polymers based on ionic liquids. *Electrochimica Acta* 50(2-3): 255-261.
  21. van de Loosdrecht AA, Beelen RH, Ossenkoppele GJ, Broekhoven MG, Langenhuijsen MM (1994) A tetrazolium-based colorimetric MTT assay to quantitate human monocyte mediated cytotoxicity against leukemic cells from cell lines and patients with acute myeloid leukemia. *J Immunol Methods* 174(1-2): 311-320.
  22. Dupont J, Scholten JD (2010) On the structural and surface properties of transition-metal nanoparticles in ionic liquids. *Chemical Society Reviews* 39:1780-1804.
  23. Peppas NA, Sahlin JJ (1989) A simple equation for the description of solute release. III. Coupling of diffusion and relaxation. *International Journal of Pharmaceutics* 57(2): 169-172.
  24. Karatas A, Baykara T (2001) Studies on indomethacin inserts prepared by water-soluble polymers: II. The relation between dissolution rate and swelling behaviour. *Farmaco* 56(3): 197-202.
  25. Singh B, Sharma V (2014) Influence of polymer network parameters of tragacanth gum-based pH responsive hydrogels on drug delivery. *Carbohydr Polym* 101: 928-940.